Int. J. Electrochem. Sci., 7 **(2012)** 5314 - 5330

International Journal of
ELECTROCHEMICAL
SCIENCE
www.electrochemsci.org

Elucidation of Dimethyldodecylphosphonate and CTAB Synergism on Corrosion and Scale Inhibition of Mild Steel in Simulated Cooling Water System

N. Dkhireche[1], *R. Abdelhadi*[1], *M. Ebn Touhami*[1,*], *H. Oudda*[1], *R. Touir*[1], *M. Elbakri*[1], *M. Sfaira*[2], *B. Hammouti*[3], *O. Senhaji*[4], *R. Taouil*[4]

[1] Laboratoire des Matériaux, d'Electrochimie et d'Environnement, Faculté des Sciences, Université Ibn Tofaîl, BP. 133 – 14000, Kénitra, Morocco.

[2] Laboratoire d'Ingénierie des Matériaux, de Modélisation et d'Environnement, LIMME, Faculté des Sciences Dhar El Mahraz, Université Sidi Mohammed Ben Abdellah, BP 1796 – 30000, Atlas – Fès, Morocco.

[3] LCAE-URAC18, Faculté des Sciences, Université Mohammed Premier, BP 717 – 60000, Oujda, Morocco.

[4] Equipe de Chimie-physique Appliquée, U.M.I., Faculté des Sciences et Techniques, Errachidia, Maroc.

[*]E-mail: mebntouhami@yahoo.fr

Received: 4 April 2012 / *Accepted:* 15 May 2012 / *Published:* 1 June 2012

The effect of dimethyldodecylphosphonate (DMDP) and Cetyltrimethylammonium bromide (CTAB) and the mixture of both (formulation), on mild steel corrosion in simulated cooling water, has been evaluated by means of electrochemical techniques such as polarization curves (I-E) and electrochemical impedance spectroscopy (EIS). Then the surface morphology was studied by scanning electron microscopy (SEM). The obtained results revealed that these compounds perform excellently as corrosion and scale inhibitors. The inhibition efficiency increases with circulation velocity rise and resisted to immersion time. Moreover, the inhibition efficiency was circa temperature-independent and retained its performance on a surface covered by corrosion products and though in very aggressive media such as 3% NaCl. These results were corroborated by SEM analyses which indicated a formation of a protective film formed on the mild steel surface by the proposed formulation.

Keywords: Scale and corrosion inhibition; Formulation; Cooling water; Synergy; Operational parameters effect

1. INTRODUCTION

The use of water as thermal fluid in cooling water system usually leads to three problems namely: scale, corrosion and biological fouling processes. These phenomena are the cause of lower

thermal efficiency of the circuit, loss of the metallic material and the growth of microorganisms in water. The economic losses caused by these problems are for the most part huge and consistent. To limit the damage, many formulations have been developed to protect circuits, piping and materials structures against this scourge [1]. The proposed formulations contain primarily inhibitors for corrosion and scale as well as biocides to decrease biofouling and microbiologically influenced corrosion.

Indeed, Srusiwan et al. [2] have studied the inhibition of mild steel corrosion in 200 mg/L NaCl solution; simulating medium of natural waters, containing a mixture of organic compounds. The use of electrochemical and spectroscopic techniques shows that the optimized formulation inhibitor (50 ppm of fatty amines + 1500 ppm of sodium sebecate) has a good corrosion inhibition for mild steel. This can be explained by the formation of a relatively compact film on metallic surface. It was also shown that the inhibition properties of this film remain independent of hydrodynamic conditions and is reinforced with the immersion time. Other formulations for treatment of industrial water based tertiary amine and carboxylic acid were also studied [3,4]. Moreover, Ramesh et al. [5,6] have developed complex formulations, for water treatment, composed by triazole phosphonate as corrosion inhibitors added with a non-oxidizing biocide (*CTAB*).

In our laboratory, several formulations were used such as sodium gluconate [7], monosaccharides [8], *TDMTAA* [9], and phosphonate monoacid [10]. The use of the phosphonic acids to protect iron and its alloys against corrosion in different environments has been reported by several researchers [11-13].

Phosphonates, originally used in water treatment, are more less susceptible to hydrolysis compared to phosphates and therefore less eutrophiants. They prevent calcium deposits on metal surfaces [14,15] and were also found to be good corrosion inhibitors [10,16,17]. Their environmental impact has been reported to be negligible at the used concentrations for corrosion inhibition [18-20].

In this direction, on the development of novel corrosion and scale formulations, dimethyldodecylphosphonate, *DMDP* and cetyltrimethylammonium bromide *CTAB* as non-oxidizing biocide, and *DMDP-CTAB* mixture were evaluated. Indeed, it is often not known whether interference between biocides and inhibitors will lead to a synergism effect or to an adverse result. To address this issue, we carried out electrochemical studies of corrosion and scale inhibition in cooling medium under similar conditions to those typically operating in industry as well as for their inhibition by chemical additive to control these processes.

2. EXPERIMENTAL DETAILS

The electrochemical study was carried out in a standard three-electrode electrolytic cell. The reference was saturated calomel electrode (SCE) and the counter electrode was a graphite bar.

The working electrode (WE) was a mild steel disc with surface area of 1.13 cm^2 and was embedded in polytetrafluoroethylene (PTFE) to avoid any infiltration of electrolyte. The WE was a rotating disc electrode and had the following composition (wt :): 0.11% C, 0.24% Si, 0.47% Mn, 0.12% Cr, 0.02% Mo, 0.1% Ni, 0.03% Al, 0.14% Cu, <0.0012% Co, <0.003% V, 0.06% W and Fe:

balance. The mild steel surface was cleaned by mechanical polishing with emery paper from 400 to 1200 grade, washed with acetone, distillated water and then dried with hot air. The simulated solution under study had the following composition: 169 ppm Ca^{2+}; 120 ppm Mg^{2+}; 150 ppm SO_4^{2-}; 460 ppm Cl^-; 230 ppm HCO_3^-; 70 ppm NO_3^- and 87 ppm Na^+. This composition represents the average concentration of salts present in the water used in Moroccan cooling water systems. The temperature and pH were adjusted to 32 ± 1 °C and 7.3 ± 0.02 respectively, which are characteristic operating conditions for these systems. The structure of dimethyldodecylphosphonate, *DMDP*, and cyltrimethylammonium bromide, *CTAB* investigated in this study is presented in Fig. 1.

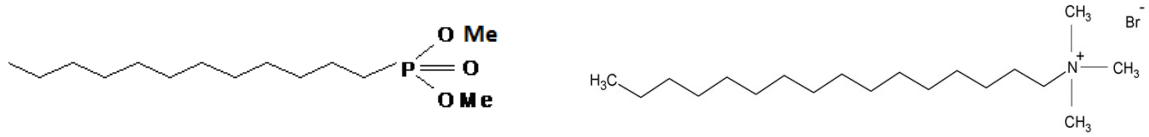

(a) **(b)**

Figure 1. Structure of dimethyldodecylphosphonate (*DMDP*) (a), and cyltrimethylammonium bromide (*CTAB*) (b)

The polarization measurements were carried out by a potentiostat (VoltaLab model PGZ100) and controlled with analysis software (Voltamaster 4) at scan rate of 1 mV s^{-1}. The WE was immersed in the test solution for one hour until a steady state open circuit potential (*E*ocp) was obtained. The rotating speed was maintained at 1000 rpm. The cathodic polarization curve was recorded by polarization from *E*ocp to negative direction under potentiodynamic conditions corresponding and under air atmosphere. After this scan, the anodic polarization curve was recorded by polarization from the *E*ocp to positive direction. The polarization curves were corrected for the ohmic drop measured by electrochemical impedance spectroscopy. All potentials are expressed with respect to SCE.

The evaluation of corrosion kinetics parameters was obtained using a fitting by Stern–Geary equation. The inhibition efficiency $IE_P\%$ was evaluated from the measured *icorr* values using the relationship (1):

$$IE_P\% = \frac{i^0_{corr} - i_{corr}}{i^0_{corr}} \times 100 \qquad (1)$$

Where i^0_{corr} and i_{corr} denote the corrosion current densities values without and with DMDP, CTAB or mixture, respectively.

The electrochemical impedance spectroscopy (EIS) measurements were performed using a transfer function analyzer (Voltalab PGZ 100), with a small amplitude AC signal (10 mV rms) over a frequency domain from 100 kHz to 10 mHz at 32°C with 5 points per decade.

Computer programs automatically controlled the measurements performed at rest potentials after an hour of immersion at *E*corr. The impedance diagrams were given in the Nyquist

representation. The inhibition efficiency was evaluated from the polarization resistance using the equation (2):

$$IE_{imp}\% = \frac{R_P - R_P^0}{R_P} \times 100 \quad (2)$$

Where R^0p and Rp are the polarization resistance values without and with inhibitors, respectively.

The electrical parameters for the impedance plots were obtained by analyzing the experimental data by means of equivalent circuits and the non-linear regression algorithm of Boukamp [21].

The examination of mild steel surface after exposure in simulated water solution with and without inhibitors was carried out using scanning electronic microscope (SEM; JEOL JSM-5500).

3. RESULTS AND DISCUSSIONS

3.1. Effect of DMDP concentration

3.1.1. Potentiodynamic polarization

The potentiodynamic polarization curves for mild steel in simulated cooling water solution at 32°C in the absence and the presence of *DMDP* at various concentrations are shown in Fig. 2. It is shown that the corrosion potential (E_{corr}) shifted to a more positive value and the corrosion current density (i_{corr}) decreased within addition inhibitor. In addition, in the absence of *DMDP*, a current plateau (800 μA cm^{-2}) appeared from −0.8 to −1.1 Vsce, attributed to the oxygen reduction reaction [22].

For the both concentrations 5×10^{-4} and 10^{-3} M, a pseudo-plate of passivity appeared in the anodic range. This a characterization of protective film formation on metallic surface. However, in the examination of cathodic range, it seems that there is no significant difference between the curves obtained with and without inhibitor. This result indicates the anodic character of *DMDP*. Then *DMDP* exert an efficient inhibitive action on the anodic dissolution of metal. It is also shown a significant decrease in the anodic current densities with increasing inhibitor concentration and reaches a minimum at 5×10^{-4} M

Electrochemical corrosion kinetics parameters, at different concentration of *DMDP*, such as corrosion potentials (E_{corr}) and corrosion current densities (i_{corr}) derived from Stern–Geary equation, as well as inhibitor efficiencies are listed in Table 1. The analysis of these results shows that the increase of *DMDP* concentration is accompanied by a reduction of current density i_{corr}, and thereby an increase in corrosion inhibition efficiency $IE_P\%$ follows. In addition, a very slight increase of i_{corr} is registered at 10^{-3} M of *DMDP*. The reduction of anodic current densities in the presence of *DMDP* can be imputed to the blocking of active sites, especially anodic ones, with the formation of protective film on the electrode surface.

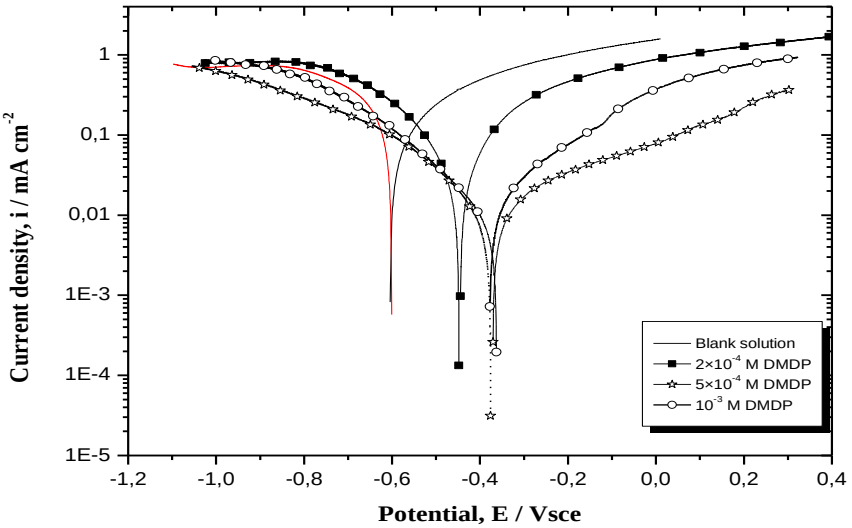

Figure 2. Polarization curves of mild steel in simulated solution without and with various concentrations of *DMDP*

Table 1. Electrochemical data obtained from the potentiodynamic curves for mild steel in simulated solution with varying concentrations of *DMDP*

Concentration / M	Ecorr / mVsce	icorr / µA cm-2	IEP%
00	-602	102	-
2×10-4	-448	22	78
5×10-4	-368	7	93
10-3	-378	10	90

Generally, adsorption is described by two main types of interaction namely physical adsorption and/or chemisorption. It depends on the metal charge and its nature, the chemical structure of organic compounds and the electrolyte nature [23,24]. It is generally assumed that chemisorption involves the share or charge transfer from the molecules onto the surface to form a coordinate type bond. Moreover, electron transfer is typical for transition metals having vacant low energy electron orbital. This transfer was enhanced by the presence of heteroatoms with free electron pairs [25,26].

3.1.2. EIS measurements

Fig. 3 shows the Nyquist plots for mild steel in simulated cooling water containing newly synthesized organic inhibitor, *DMDP*, at different concentrations after one hour of immersion time at corrosion potential, E_{corr}. It is shown that these diagrams are composed of two loops. At high frequencies, the first loop can be attributed to the formed film adsorption by the inhibitor molecules, and at low frequencies is assigned to the relaxation of double layer in parallel with the charge transfer resistance. Nevertheless, it is difficult to attribute this time constant to a pure charge transfer and therefore, we use a polarization resistance. It is note that an increasing inhibitor concentration leads to

an increase in the impedance value. This result reflects the influence of organic inhibitor on the process at the interface metal-solution. EIS spectra were analyzed using the equivalent circuit in Fig. 4. The impedance parameters derived from these figures are given in Table 2. R_s is the solution resistance, R_{ct} is the charge transfer resistance, R_f is the film resistance, *CPE1* is considered as a model of double layer capacitance (C_{dl}) supposing that H_2O and other ions adsorbed on the surface of mild steel, and *CPE2* as a model of inhibitor film (C_f). It is shown that the R_p values increases with increasing of *DMDP* concentration indicating that the inhibition efficiency increases. This increase results from a decrease in local dielectric constant and/or an increase in the thickness of the electrical double layer, suggesting that the phosphonate molecules adsorbs on the metal/solution interface [27]. In addition, the changes in R_p, C_f, R_f values were caused by the gradual replacement of water molecules and other ions originally adsorbed on the surface by adsorption of the organic molecules on the metal/solution interface leading to a protective film against the dissolution reaction for mild steel [28]. However, this result can be explained by the fact that the corrosion reaction on the electrode surface was inhibited by the absorbed inhibitor [29]. Furthermore, the values of inhibition efficiencies obtained from EIS were compared and close to those obtained by polarization measurements.

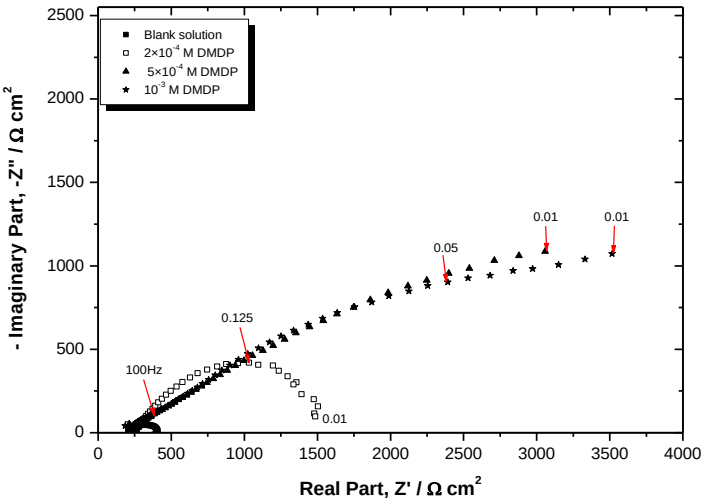

Figure 3. Nyquist plot for mild steel in simulated solution in the presence of different concentrations of *DMDP*

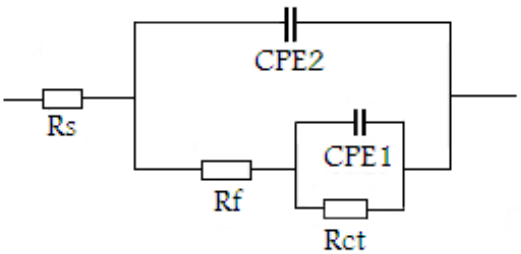

Figure 4. The corresponding equivalent circuits used in modeling the electrochemical impedance spectra data in the presence of *DMDP* inhibitor

Table 2. The electrochemical parameters for mild steel in simulated solution in the presence of different concentration of *DMDP* inhibitor

Concentration / M	Rf / Ω cm2	Cf / µF cm-2	Rp / Ω cm2	Cdl / µF cm-2	IEimp%
00	-	-	200	1710	-
2×10-4	-	-	1324	724	84
5×10-4	510	2.3	6015	86	96
10-3	470	3.7	6010	138	96

3.2. Effect of CTAB addition: Development of a new inhibitory formulation

We examined the effect of adding a non-oxidizing biocide *CTAB* on the inhibition efficiency of *DMDP*. We recall that the *CTAB* is used to decrease biological fouling. For example, previous studies have shown that this biocide has very good inhibition efficiency against bacterial growth when added at 15 ppm of concentration [5,6]. For this purpose, we tested the effect of this biocide. Fig. 5 shows the electrochemical behavior of mild steel in simulated solution in the presence of 5×10^{-4} M *DMDP* + 15 ppm *CTAB*. It is note that the diagram of *CTAB*, consists of two loops well separated, one at high frequency and the other at low frequencies previously reported [30]. Table 3 shows the electrochemical parameters calculated from EIS measurements. It is note that the *CTAB* appears like a corrosion inhibitor and has inhibition efficiency about 52 %. This result is in agreement with literature work [5,6,30].

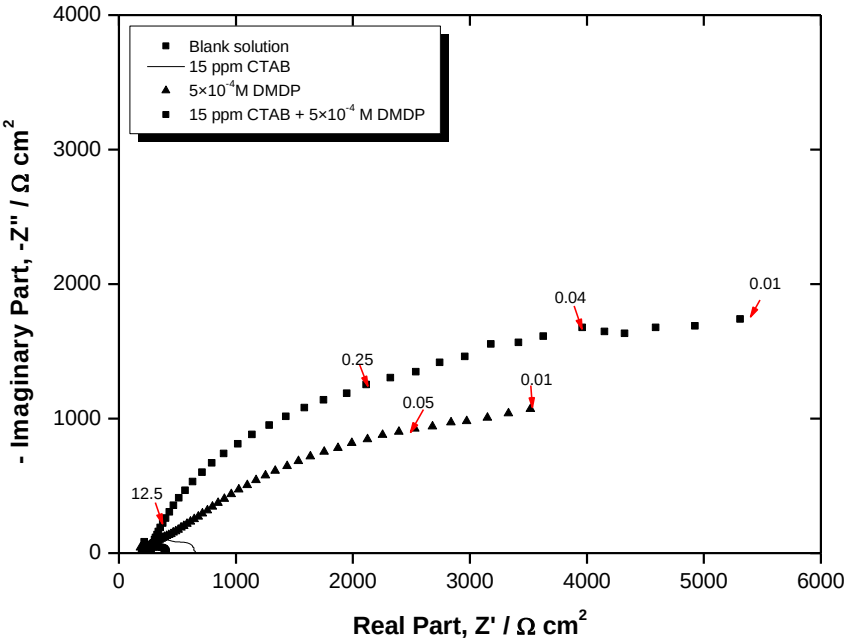

Figure 5. Impedance spectra of mild steel surface in simulated solution with 5×10^{-4} M *DMDP* + 15 ppm of *CTAB* and mixture of both

Table 3. Impedance parameters obtained on mild steel surfaces in the simulated solution at different concentrations of *DMDP* and *CTAB* compounds and synergism parameter S_θ calculated from EIS measurements

Concentration	Rp / □□cm²	Cdl / µF cm-2	Θ	IEimp%	Sθ
00	200	1710	-	-	-
15 ppm CTAB	420	1123	0.5238	52	-
5×10-4 M DMDP	6013	86	0.9667	96	-
5×10-4 M DMDP + 15 ppm CTAB	11600	221	0.9827	98	1.12

On the other hand, the presence of *CTAB* with *DMDP* clearly increases the polarization resistance R_p. It is increase from 6013 Ω cm^2 in the presence of *DMDP* only to 11600 Ω cm^2 in the presence of both products (mixture). This behavior was attributed to the synergistic effect between these compounds.

Aramaki et al. [31-33] have proposed two types of joint adsorption namely competitive and cooperative. In competitive adsorption, the anion and cation are adsorbed at different sites on the metal surface, while in cooperative adsorption, the anion is chemisorbed on the surface and the cation is adsorbed on a layer of the anion. The synergism parameter, S_θ, was calculated from the impedance data using the following relationships:

$$S_\theta = (1 - IE_{1+2})/(1 - IE'_{1+2}) \quad (3)$$

$$IE_{1+2} = IE_1 + IE_2 - IE_1 \times IE_2 \quad (4)$$

$$IE'_{1+2} = 1 - [(1/R_{P1+2})/(1/R_{P0})] \quad (5)$$

IE_{1+2} and IE'_{1+2}: The calculated and measured inhibition efficiencies of mixture, respectively.
IE_1 and IE_2: The inhibition efficiency of each compound separately calculated from the R_p.
$R_{P\,1+2}$: polarization resistance in the presence of mixture.
$R_{P\,0}$: polarization resistance in the absence of both compounds.

Table 3 gives the S_θ value which is more than unity suggesting that the enhanced inhibition efficiency caused by the addition of *CTAB* ions to *DMDP* is only due to the synergistic effect. The synergistic inhibition effect, in the present study, can be explained as follows: The strong chemisorption of *CTAB* ions on the metal surface is responsible for the synergistic effect of *CTAB* combination with *DMDP*.

The *DMDP* is then adsorbed by coulombic attraction on metallic surface where *CTAB* ions are already adsorbed (cooperative adsorption). Stabilization of adsorbed *CTAB* ions with the inhibitor leads to great surface coverage and thereby greater inhibition efficiency.

3.3. Effect of operational parameters on the formulation performance

3.3.1. Effect of Temperature

Temperature, which is an essential parameter in the operation of cooling water systems, was also taken into account. In a great majority of cases, exposure of a material in aggressive solution at high temperature results in a uniformly degradation over the entire metallic surface. Fig. 6 represents the potentiodynamic polarization curves for mild steel in simulated water system containing 5×10^{-4} M of *DMDP* + 15 ppm of *CTAB* at different temperatures ranging from 32 to 62 °C.

It is seen that the rise of temperature does not practically affect the general appearance of the cathodic curves, the corrosion potential shifts towards more negative values and also increases the anodic current at potentials below 0 Vsce. Beyond this value, the curves become adjacent and relatively lower anodic currents corresponding to 32 °C. The parameters extracted from these curves at the studied temperatures are given in Table 4.

It is note that the corrosion rate increases with increasing temperature. This effect is attributed to the increase in the amount of diffusion oxygen with the temperature rise [34]. However, in the present study, the inhibition efficiency appears to be is practically temperature-independent in the range of temperature explored 32-62 °C. Therefore, this formulation (*DMDP + CTAB*) is stable and very effective at high temperatures, at least in the temperature range explored.

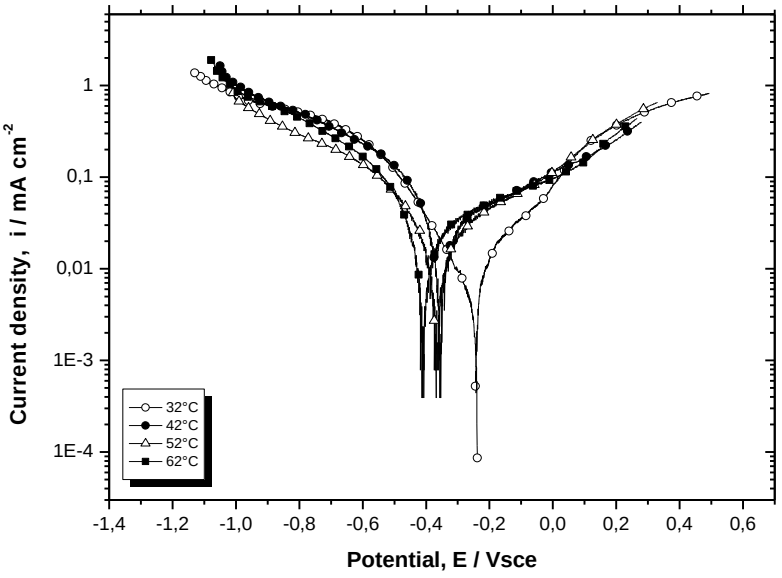

Figure 6. Polarization curves of mild steel in simulated solution with 5×10^{-4} M of *DMDP* + 15 ppm of *CTAB* at various temperatures (Ω = 1000 rpm)

The Arrhenius plots; i.e., the corrosion current density logarithm versus reciprocal temperature T^{-1} is given in Fig. 7. These plots are straight lines and the slope of each one gives its activation energy E_a. It is observed that for the mild steel corrosion in free simulated solution, the E_a value was found equal to 14.52 kJ mol^{-1}. In the presence of mixture, the E_a value is higher and equal to 25.41 kJ mol^{-1}.

According to Gomma [35], the kinetics of such corrosion process acquires the character of a diffusion process in which at lower temperature the quantity of inhibitor present at the metal surface is greater than that at higher temperatures. However, the negative slope of Arrhenius coordinates indicates that the organic compounds are adsorbed on metallic surface [36].

Table 4. Electrochemical parameters of mild steel in simulated solution with 5 10^{-4} M *DMDP* + 15 ppm *CTAB* at different temperatures (Ω = 1000 rpm)

Solution	Temperature / °C	Ecorr / mVsce	icorr / µA cm-2	IEP%
Bank solution	32	-605	102	-
	42	-621	121	-
	52	-695	151	-
	62	-698	162	-
Mixture	32	-239	5	95
DMDP + CTAB	42	-351	7	94
	52	-368	8	94
	62	-414	13	92

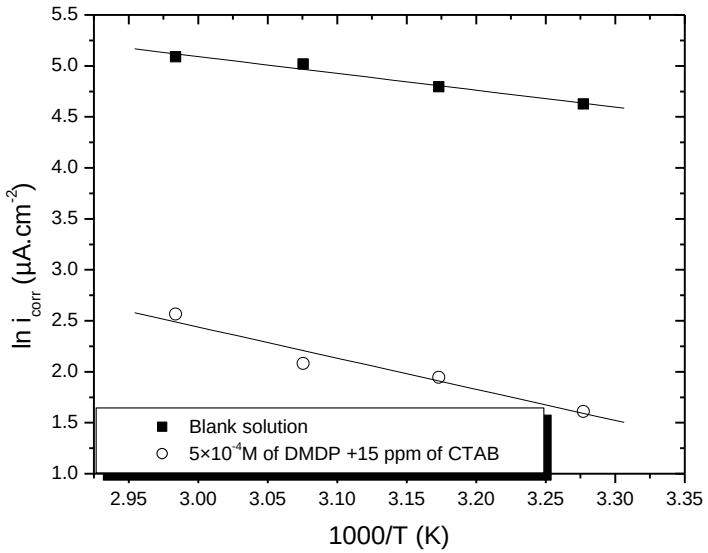

Figure 7. Relation between corrosion rate and reciprocal of temperature in the absence and the presence of mixture

3.3.2. Effect of hydrodynamic conditions

Fig. 8 shows the potentiodynamic polarization curves at different water circulation velocity over open circuit potential in the presence of 5×10^{-4} M of *DMDP* + 15 ppm of *CTAB*. The parameters evolution with different rate of electrode is summarized in Table 5. It is shown that the cathodic current densities increase while the anodic current densities decrease and the corrosion potentials are shifted towards more anodic with rise of the electrode rotation rate. The same behavior was obtained

by N. Srisuwan et al. [2] for mild steel in 200 ppm NaCl medium. Thus, the increase in the cathodic current density is probably attributed to the increase on the diffusion oxygen to metallic surface. The decrease in the anodic current densities with increasing rotation rate is an unusual behavior; previous studies have shown this behavior and have attributed it to the chemical composition and morphology of the formed film on metallic surface [37].

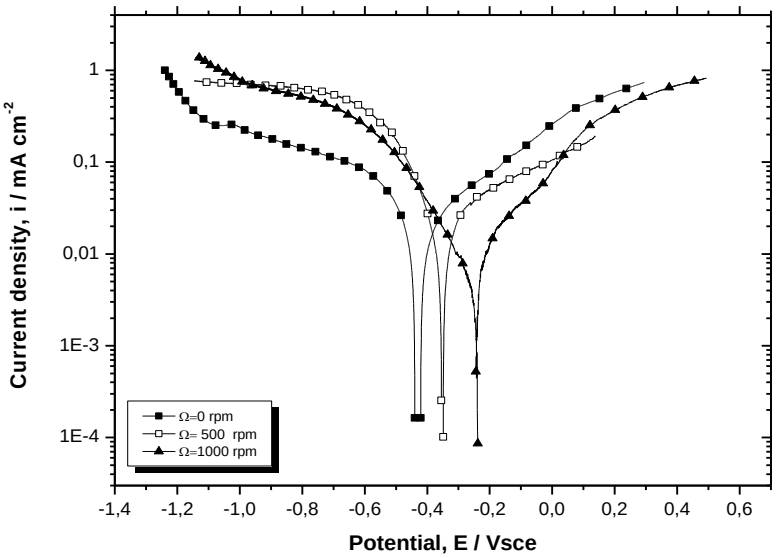

Figure 8. Polarization curves of mild steel in simulated solution with mixture inhibitor formulation at different rotation rates

Table 5. Electrochemical parameters of mild steel in simulated solution with 5×10^{-4} M *DMDP* + 15 ppm *CTAB* at various rotation rates

Rotation rate / rpm	Ecorr / mVsce	icorr / µA cm-2	IEP%
00	-430	24	76
500	-350	22	78
1000	-240	5	95

To confirm the influence of hydrodynamic effect on the inhibition efficiency of formulation, EIS was carried out at different rotation rates, after one hour of immersion time at corrosion potential. Typical Nyquist diagrams obtained are shown in Fig. 9. The impedance diagrams are composed of two loops for all rotation sweeps and are not perfect semicircles. Table 6 gives the deduced impedance parameters. From these diagrams, it can be seen that the mass transport plays a crucial role in the interface process and the hydrodynamic effect is similar to the concentration one. This may be explained by a possible bring of more molecules inhibitors at the interface.

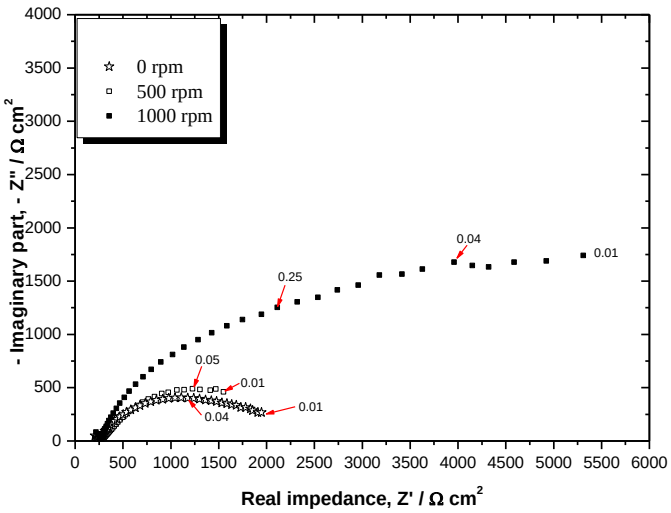

Figure 9. Nyquist plots of mild steel in simulated solution with 5×10^{-4} M of *DMDP* + 15 ppm of *CTAB* at different rotation rates

Table 6. Electrochemical parameters and coverage surface values of mild steel in simulated solution with 5×10^{-4}M *DMDP* + 15 ppm *CTAB* at various rotation rates

Rotation rate / rpm	Rp / □ cm²	Cdl / □F cm-²	IEimp%
00	2310	757	91
500	2480	226	92
1000	11600	221	98

In fact, the hydrodynamic effect seems to promote and favor the formation of a less permeable protective layer and simplified the movement of the mixture molecules to metallic surface in order to form a layer with a higher resistance. These results join other studies, in fact, Ochoa et al. [38] studied the behavior of mild steel / 200 ppm NaCl interface in the presence of an optimized formulation (50 ppm of fatty amine added of 200 ppm of phosphonocarboxylic salts). They showed that the electrode rotation rate determines the inhibition properties of film, since lower densities are recorded with increasing the electrode rotation rate. These studies were confirmed by XPS analysis of the surface. Indeed, the increase in rotation rate of the electrode promotes the formation of chelate and consequently greater inhibition properties of the formed film.

3.3.3. Effect of immersion time

Fig. 10 shows the impedance spectra at different immersion time in simulated cooling water containing the formulation with 1000 rpm of the electrode rate. It is note that the increasing of immersion time does not practically affect the diameter loops. The impedance results suggest that immersion time does not influence significantly the inhibition process and the proposed formulation retains its performance despites for higher periods of immersion time in the aggressive solution.

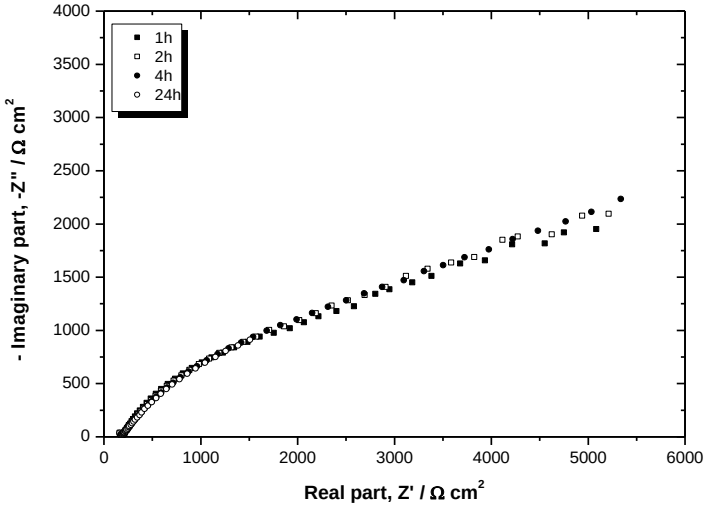

Figure 10. Electrochemical impedance spectra obtained after different immersion times in simulated cooling water with 5×10^{-4}M *DMDP* + 15 ppm *CTAB* (T = 32°C; Ω = 1000 rpm).

3.3.4. Effect of corrosion products

To collect more information on the mechanism of formulation molecules action, the possible interaction between the corrosion products and adsorbed film by (5×10^{-4} M *DMDP* + 15 ppm *CTAB*), an investigation has been made using electrochemical impedance spectroscopy. For this purpose, we examined the addition effect of inhibitor mixture at different immersion times of mild steel after 2 h immersion in the corrosive solution (Fig. 11). The electrochemical data resulting from these diagrams are illustrated in Table 7. It is note that the formulation has a high efficiency; ca. 86% from the first hour after addition of the inhibitor mixture. This efficiency tends to strengthen with increasing immersion time. About this result, we can conclude that the investigated formulation provides good protection despite the presence of corrosion products on mild steel surface. This shows that the studied formulation is also valid for cooling water protection already damaged.

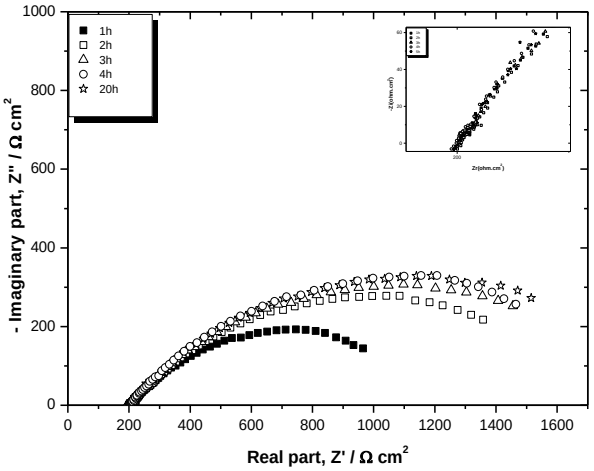

Figure 11. Impedance Nyquist plots of mild steel after 2 h of immersion in corrosive solution and after different adding the mixture formulation (T = 32 °C and Ω = 1000 rpm)

Table 7. Impedance parameters of mild steel in simulated cooling water after different additions of the mixture formulation (T = 32°C and Ω = 1000 rpm)

Immersion time / h	Rs / □ cm²	Rp / □ cm²	Cdl / □F cm-²	IEimp%
1	200	1381	1557	85.5
2	210	1660	1462	88
3	200	1820	1376	89
4	200	1907	1150	89.5
20	200	1984	1982	90

3.3.5. Effect of chloride ions: Study in 3% NaCl medium

In order to evaluate the inhibition potential of the mixture, we choose another more aggressive medium such as 3% NaCl.

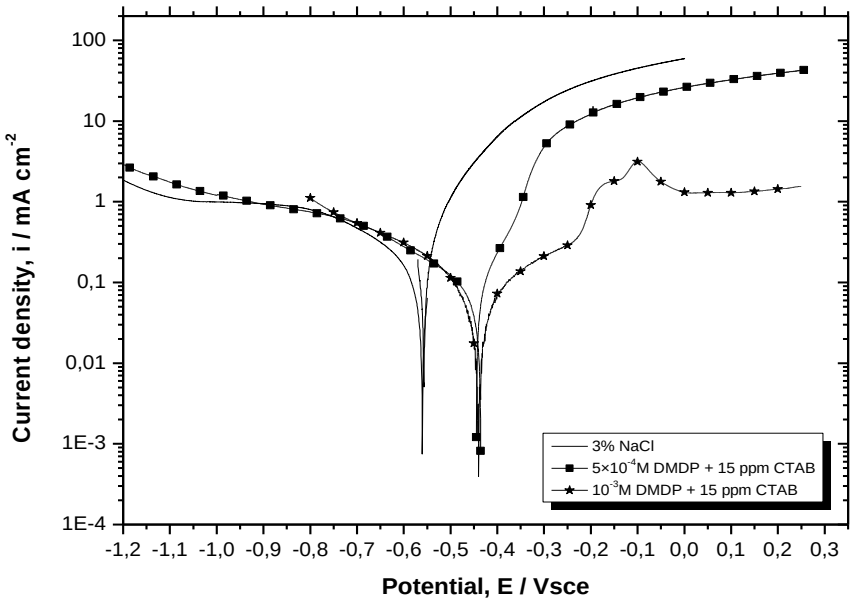

Figure 12. Potentiodynamic polarization curve of mild steel in 3% NaCl solution with different concentration of DMDP and in the presence of 15 ppm of *CTAB* (T = 32°C, Ω = 1000 rpm)

The potentiodynamic polarization curves were carried out in turn to characterize the corrosion behavior of mild steel immersed for 1 h, at free corrosion potential, in 3% NaCl medium containing 5×10^{-4} M *DMDP* + 15 ppm *CTAB*. The obtained results are given in Fig. 12. It is seen that the addition of mixture moves the corrosion potential E_{corr} to more positive potentials and reduces remarkably the anodic current density. This effect is more pronounced in the presence of the formulation at double concentration of *DMDP*; i.e., at 10^{-3} M. At this concentration we observe for the anodic range, a pseudo plate neighbor -0.3 Vsce. Moreover, for the anodic over-potential, current plate on a wide potential range (ca. 300 mVsce) was appeared. By cons, we do not notice a big change in the cathodic

range. The electrochemical parameters summarized in Table 8, show that this formulation provides very good efficiency for corrosion (95,5%) and keeps its performance in very aggressive solution.

Table 8. Electrochemical parameters of mild steel in 3% NaCl solution with different concentrations of *DMDP* and in the presence of 15ppm of *CTAB* (T = 32°C, Ω = 1000 rpm)

Concentration	Ecorr / mVsce	icorr / µA cm-2	IEP%
00	-555	690	-
5 ×10-4 DMDP + 15 ppm CTAB	-443	78	89
10-3 DMDP + 15 ppm CTAB	-440	31	95.5

3.4. Scanning electron microscopy, SEM analyses

Fig. 13 shows the scanning electronic microscopy (SEM) images of mild steel surface immersed in simulated solution during one day in the absence and presence of 5×10^{-4} *DMDP* + 15 ppm of *CTAB.*

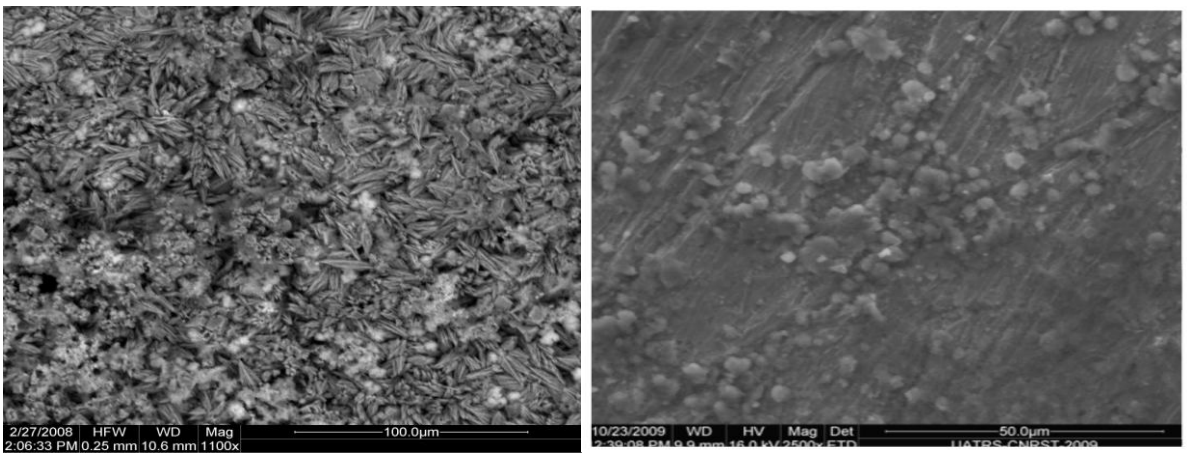

A **B**

Figure 13. SEM pictures of mild steel surface after 24 h immersion in simulated cooling water: (a) without formulation and (b) with mixture formulation

Furthermore, the SEM image in the presence of 5×10^{-4} M *DMDP* + 15 ppm *CTAB* (Fig. 13b) shows a large area free of corrosion and scale products and reveals the presence of globular species. In this case, EDAX analysis (Fig. 14b) showed again a height decreasing of calcium peaks, the presence of phosphorus, nitrogen and oxygen peaks indicating that the formulation molecules are adsorbed on metallic surface forming a compact film. These results show that this formulation plays both scale and corrosion inhibitor.

In other respects, studies were conducted by FTIR and SEM to determine the mechanism action of phosphonate to prevent mild steel corrosion in a neutral medium [5,6]. These studies have shown that the inhibition character of these compounds is due to the formation of a compact protective film and adherent, consisting mainly of Fe-phosphonate complex. Thus, the SEM analysis perfectly confirms the results obtained by electrochemical studies.

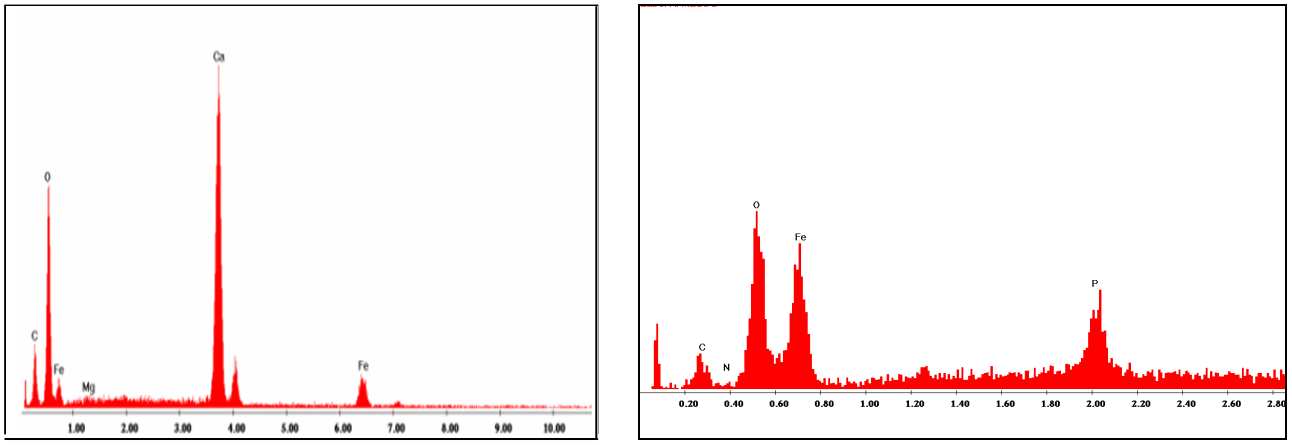

A **B**

Figure 14. EDAX analysis of mild steel electrode surface after 24 h immersion in simulated cooling water: (a) without formulation and (b) with 5×10^{-4} M *DMDP* + 15 ppm *CTAB*

4. CONCLUSION

The corrosion and scale inhibition of mild steel by *DMDP* and its mixture with *CTAB* were studied by electrochemical measurements and SEM analyses.

The results show that *DMDP* inhibitor has the ability of reducing the corrosion rate of mild steel in Moroccan simulated cooling water and it acts as anodic inhibitor. The increasing of *DMDP* concentration has a positive influence on its performance as a corrosion inhibitor and reaches a maximum at 5×10^{-4} M. This effectiveness is confirmed by electrochemical impedance spectra.

The biocide *CTAB* added to *DMDP* performance was attributed to the synergistic effect between these compounds (formulation). The inhibition efficiency of this formulation has low temperature and immersion time dependence and increases with rotation rate of electrode.

In addition, the formulation keeps its effectiveness despites in more aggressive medium such as 3% NaCl. The mechanism action of the molecules formulation is based on cooperation adsorption forming a compact film and the adsorption process is corroborated by scanning electron microscopy.

References

1. F. Moran, Traitement des eaux. Ecole thématique : Prévention et lutte contre la corrosion Tome IV, Anglet, 2002.

2. N. Srisuwan, Thèse de Doctorat, Institut National Polytechnique de Toulouse (France), 2008.
3. P. Bommersbach, C. Alemany-Dumont, J.P. Millet, B. Normand, *Electrochim. Acta*, 51 (2005) 1076.
4. P. Bommersbach, C. Alemany-Dumont, J-P Millet, B. Normand, *Electrochim. Acta*, 51 (2006) 4011.
5. S. Ramesh, S. Rajeswari and S. Maruthamuthu, *Mater. Lett*., 57 (2003) 4547.
6. S. Ramesh and S. Rajeswari, *Corros. Sci*., 47 (2005) 151.
7. R Touir, M. Cenoui, M. EI Bakri, M. Ebn Touhami, *Corros. Sci*., 50 (2008) 1530.
8. R. Touir, N. Dkhirech, M. Ebn Touhami, M. Lakhrissi, B. Lakhrissi, M. Sfaira, *Desalination*, 249 (2009) 922.
9. M. Cenoui, N. Dkhirech, O. Kassou, M. Ebn Touhami, R. Touir, A. Dermaj, N. Hajjaji, *J.Mater. Environ. Sci.*, 1 (2010) 84.
10. R. Touir, N. Dkhireche, M. Ebn Touhami, M. Sfaira, O. Senhaji, J.J. Robin, B. Boutevin, M. Cherkaoui, *Mater. Chem. Phys*., 122 (2010) 1.
11. J.L. Frang, Multiple Complex Electroplating, *Defence Industry Press, Beijing, China*, (1983) 273.
12. H. Amar, J. Benzakour, A. Derja, D. Villemin, B. Moreau, T. Braisaz, A. Tounsi, *Corros. Sci*., 50 (2008) 124.
13. My R. Laamari, J. Benzakour, F. Berrekhis, A. Derja, D. Villemin, Les technologies de laboratoire, Volume 5, N° 20, (2010).
14. G. Trabanelli, V. Carassiti, Corros. Sci. Techno., Plenum Press, New York, 1970.
15. B. Zhang, L. Zhang, F. Li, W. Hu, P.M. Hannam, *Corros. Sci.*, 52 (2010) 3883.
16. H.S. Awad, Turgoose, *Corrosion*, 60 (2004) 1168.
17. T. Du, J. Chen, D. Cao, *J. Mater. Sci*., 36 (2001) 3903.
18. H.S. Awad, *Anti-Corros. Meth. Mater*., 52 (2005) 22.
19. J. Jaworska, H.V. Genderen-Takken, A. Hanstveit, E. Plassche, Feijtel, *Chemosphere*, 47 (2002) 655.
20. B. Yactine, F. Ganachaud, O. Senhaji, B. Boutevin, *Macromolecules*, 38 (2005) 2230.
21. A.Bouckamp, Users Manual Equivalent Circuit, Ver. 4.51, (1993).
22. O'M. Bockris, A.K.N. Reddy, 'Modern Electrochemistry' (Plenum, New York, (1970)2230.
23. O. Olivares, N.V. Likhanova, B. Gomez, J. Navarrete, M.E. Llanos-Serrano, E. Arce, J.M. Hallen, *Appl. Surf. Sci*. 252 (2006) 2894.
24. Popova, E. Sokolova, S. Raicheva, M. Christov, *Corros. Sci*., 45 (2003) 33.
25. M. Lagrenee, B. Mernari, M. Bouanis, M. Traisnel, F. Bentiss, *Corros. Sci*., 44 (2002) 573.
26. J. Vosta, J. Eliasek, *Corros. Sci.*, 11 (1971) 223.
27. H. Ashassi-Sorkhabi, B. Shaabani, D. Seifzadeh, *Appl. Surf. Sci*. 239 (2005) 154.
28. W. Kohn, A.D. Becke, R.G. Parr, *J. Phys. Chem*. 100 (1996) 12974.
29. R. J. Zhang, X.L. Gong, H.H. Yu, M. Du, *Corros. Sci*., 53 (2011) 3324.
30. R. Touir, N. Dkhireche, M. Ebn Touhami, M. El Bakri, A. Rochdi, R. A. Belakhmima, *J. Saudi Chem. Soc.*, (2011) DOI: 10.1016/j.jscs.2011.10.020.
31. K. Aramaki, N. Hackerman, *J. Electrochem. Soc.*, 134 (1987) 1896.
32. K. Aramaki, N. Hackerman, *Corros. Sci.*, 27 (1987) 487.
33. K. Aramaki, H. Nishihara, *J. Electrochem. Soc*., 134 (1987) 1059.
34. Y. Gonzalez, M.C. Lafont. N. Pébère, G. Chatainier, J. Roy, T. Bouissou, *Corros. Sci*., 37 (1995).
35. G.K. Gomma, M.H. Wahdan, *Mater. Chem. Phys*., 39 (1991) 211.
36. V. Branzoi, F. Branzoi, M. Baibarac, *Mater. Chem. Phys*., 65 (2000) 288.
37. N. Srisuwan, N. Ochoa, N. Pébère, B. Tribollet, *Corros. Sci*., 50 (2008) 1245.
38. N. Ochoa, F. Moran, N. Pébère, B. Tribollet, *Corros. Sci*. 47 (2005) 593.